

A Novel Method for Removing the Cyclic Frequency Shift due to the Earth's Motion about the Sun from Astronomical Continuous-Wave Data

Curtis Rau, Colin Gordon, David Witalka, and Samuel Akwei-Sekyere
Michigan State University

-CURTIS MAKES A TEST CHANGE In this paper we will introduce the Gustafson Algorithm for removing frequency/phase modulation from a signal. This method is powerful because it works in the frequency rather than time domain (explain why this is an advantage). Here we will focus on its applications to LIGO, but there are many applications. Some other examples are: -Radio wave astronomy -Communications systems using FM? -What are some other possible applications??

-we are given time series data. -we are looking for phase modulated gravitational waves. -form of phase modulation depends on the nature of the binary orbit. [5] [2] [1] [3] [4]

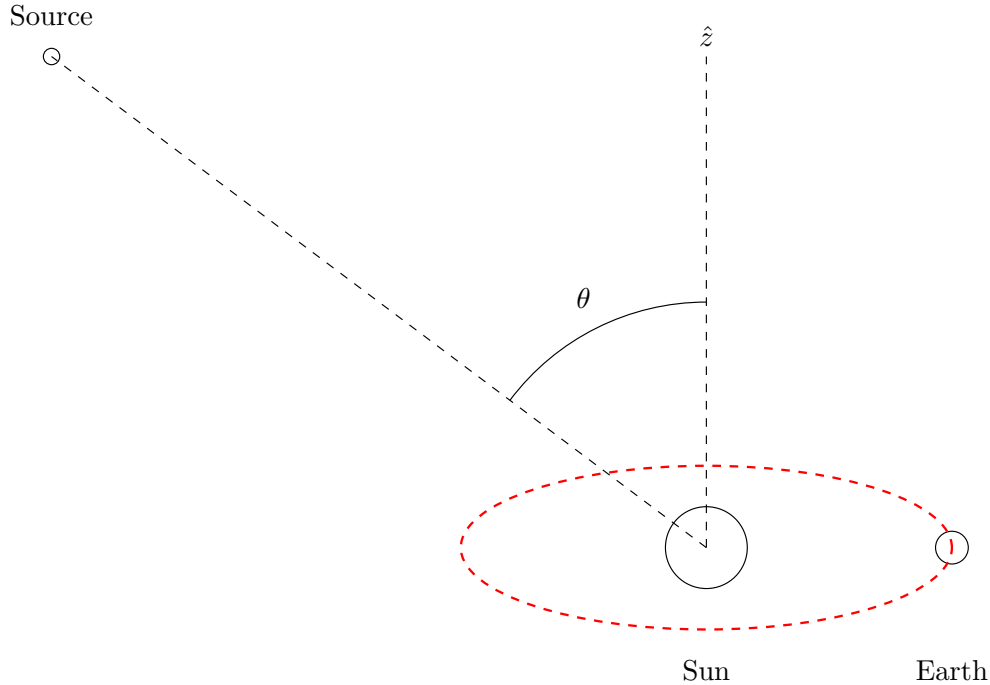


FIG. 1

– Cover Page

I. INTRODUCTION

– INTRODUCTION TO LIGO AND GRAVITATIONAL RADATION HERE –

Sources of continuous monochromatic (one frequency) gravitational radiation are predicted to exist; at least sources whose frequency wanders over many periods []. If they do exist they are apparently very low intensity as viewed from earth because none have been observed to date []. One phenomena may be (significantly??) repressing the amplitude of these signals as seen from Earth. This would be frequency modulation. When a wave is frequency modulated, its power is distributed amongst an infinite number of sidebands which are the frequencies measured when taking Fourier Transform of the data that comes from the sinusoidal phase shift due to the Doppler effect from Earth's motion relative to the source. There are two reasons to believe frequency modulation is truly occurring (reword).

Recently the discovery of gravitational waves was announced. We have reason to believe the most numerous sources of gravitational waves in the universe are compact stars (like Black holes and Neutron Stars). These stars are expected to emit single frequency waves over very long periods of time. It is also believed that roughly half of all neutron stars are in binary systems, ie. two of them orbiting around each other. This phase modulates the signal which has the effect of reducing the power in the carrier frequency and distributes it into higher and lower harmonics. This spreads out the power of the signal over a range of frequencies which makes it harder to detect these waves. Especially because there is a high noise to signal ratio in the LIGO data.

To calculate frequency observed for our wave we need to think about the source as an object that is Megaparsecs away (potentially in other galaxies). they are so far that their Spherical coordinate will not change significantly and the object will move relative to the sun with nearly constant velocity over the time we collect data. This means that the sun will see the monochromatic wave produced by the source as monochromatic. Based on this and that the waves travel at the speed of light can write the wave as a lorentz invariant 4 vector.

-The equivalence of the two ways of looking at it. -The boost is in the arbitrarily chosen x direction, and the velocity is with respect to the sun's frame of rest.

We introduce some variables: Γ is the modulation index, ω_e is the angular frequency of the Earth's rotation about the Sun, ω_0 is the frequency of the wave to be detected, ϕ_0 is the phase of the wave to be detected at $t = 0$, ϕ_e is the relative phase difference between the Earth's rotation about the Sun and the wave to be detected.

– – DEFINE : $K, \gamma, \beta, k, \theta, h_0$

$$\mathbf{K} = \begin{pmatrix} \gamma & -\gamma\beta & 0 & 0 \\ -\gamma\beta & \gamma & 0 & 0 \\ 0 & 0 & 1 & 0 \\ 0 & 0 & 0 & 1 \end{pmatrix} \begin{pmatrix} 1 & 0 & 0 & 0 \\ 0 & -\sin(\omega_e t + \phi_e) & \cos(\omega_e t + \phi_e) & 0 \\ 0 & -\cos(\omega_e t + \phi_e) & -\sin(\omega_e t + \phi_e) & 0 \\ 0 & 0 & 0 & 1 \end{pmatrix} \begin{pmatrix} \omega_0/c \\ -k \sin \theta \\ 0 \\ -k \cos \theta \end{pmatrix} \quad (1)$$

$$= \begin{pmatrix} \gamma(\omega_0/c - \beta k \sin \theta \sin(\omega_e t + \phi_e)) \\ \gamma(-\beta\omega_0/c + k \sin \theta \sin(\omega_e t + \phi_e)) \\ \gamma k \sin \theta \cos(\omega_e t + \phi_e) \\ -k \cos \theta \end{pmatrix} \quad (2)$$

So the new instentaneous frequency in the earth frame is

$$\omega(t) = \omega_0 \gamma (1 - \beta \sin \theta \sin(\omega_e t + \phi_e)) \quad (3)$$

phase is the time integral of frequency so the expression for the wave we are looking for is the real part of

$$h(t) = h_0 e^{i(\omega' t + \Gamma \cos(\omega_e t + \phi_e))} \quad (4)$$

$$\omega' = \gamma \omega_0 \quad (5)$$

$$\Gamma = \frac{\gamma \beta \omega_0 \sin \theta}{\omega_e} \quad (6)$$

-An important question to ask is what range of values could Γ take on?

-this is a frequency modulated wave -notice that Γ is a function of only the azmuthal angle of the source with respect to the normal of the gallactic plane.

II. THE GUSTAFSON ALGORITHM

It would be nice to have an algorithm that does the following:

$$h_0 e^{i(\omega_0 t + \phi_0 + \Gamma \cos(\omega_1 t + \phi_1))} \rightarrow h_0 \delta(\omega_0) \delta(\omega_1) \delta(\Gamma) \quad (7)$$

Previous methods have utilized, where $f(t)$ is the data.

$$h_0 e^{i(\omega_0 t + \phi_0 + \Gamma \cos(\omega_1 t + \phi_1))} = f(t) \quad (8)$$

$$h_0 e^{i\phi_0} e^{i\omega_0 t} = f(t) e^{-i\Gamma \cos(\omega_1 t + \phi_1)} \quad (9)$$

$$h_0 e^{i\phi_0} \mathcal{F}_t [e^{i\omega_0 t}] = \mathcal{F}_t [f(t) e^{-i\Gamma \cos(\omega_1 t + \phi_1)}] \quad (10)$$

define $F_t[f(t)](\omega) = \hat{f}(\omega)$, and invoking the convolution theorem

$$\frac{h_0 e^{i\phi_0}}{\sqrt{2\pi}} \delta(\omega_c - \omega) = \hat{f}(\omega) \star F_t [e^{-i\Gamma \cos(\Omega t + \phi)}] \quad (11)$$

invoking the Jacobi-Anger Expansion which has the form []:

$$e^{iz \cos(\theta)} = \sum_{n=-\infty}^{\infty} e^{in\pi/2} J_n(z) e^{in\theta} \quad (12)$$

so equation (2) becomes

$$\frac{h_0 e^{i\phi_0}}{\sqrt{2\pi}} \delta(\omega - \omega_0) = \hat{f}(\omega) \star \mathcal{F}_t \left[\sum_{n=-\infty}^{\infty} e^{in\pi/2} J_n(-\Gamma) e^{in(\omega_1 t + \phi_1)} \right] \quad (13)$$

Bessel Functions have the properties

$$J_n(-z) = (-1)^n J_n(z) \quad (14)$$

so

$$\mathcal{F}_t \left[\sum_{n=-\infty}^{\infty} e^{in\pi/2} J_n(-\Gamma) e^{in(\omega_1 t + \phi_1)} \right] = \sum_{n=-\infty}^{\infty} (-1)^n e^{in\pi/2} e^{in\phi_1} J_n(\Gamma) \mathcal{F}_t [e^{in\omega_1 t}] \quad (15)$$

$$= \frac{1}{\sqrt{2\pi}} \sum_{n=-\infty}^{\infty} e^{in(\phi_1 - \pi/2)} J_n(\Gamma) \delta(\omega - n\omega_1) \quad (16)$$

where we have used $(-1)^n i^n = (-i)^n = e^{-in\pi/2}$, and the linearity of the Fourier Transform $F_t[f+g] = F_t[f] + F_t[g]$. The Fourier transform of this is

$$h_0 e^{i\phi_0} \delta(\omega - \omega_0) = \hat{f}(\omega) \star \left[\sum_{n=-\infty}^{\infty} e^{in(\phi_1 - \pi/2)} J_n(\Gamma) \delta(\omega - n\omega_1) \right] \quad (17)$$

so performing the convolution

$$\hat{f}(\omega) \star \delta(\omega - n\omega_1) = \int \hat{f}(\omega - \tilde{\omega}) \delta(\tilde{\omega} - n\omega_1) d\tilde{\omega} \quad (18)$$

$$= \hat{f}(\omega - n\omega_1) \quad (19)$$

which brings us to the almost final answer:

$$h_0 e^{i\phi_0} \delta(\omega - \omega_0) = \sum_{n=-\infty}^{\infty} e^{in(\phi_1 - \pi/2)} J_n(\Gamma) \hat{f}(\omega - n\omega_1) \quad (20)$$

but for later convenience let's have $n \rightarrow -n$. We will use the other property of the Bessel Functions: []

$$J_{-n}(z) = (-1)^n J_n(z) \quad (21)$$

Which brings us to the Gustafson Algorithm (someone should check this out before we submit the paper):

$$h_0 e^{i\phi_0} \delta(\omega - \omega_0) = \sum_{n=-\infty}^{\infty} e^{-in(\phi_1 + \pi/2)} J_n(\Gamma) \hat{f}(\omega + n\omega_1) \quad (22)$$

This algorithm has been implemented in the past to demodulate the carrier frequency to recover the true amplitude [?].

This algorithm in its current form cannot be used on real data because it assumed a complex waveform. This assumption allowed for a clean demodulation, which is spoiled if one takes the real of this function. This is due to the nonlinearity (is this the correct term) of the real operator as demonstrated by

$$\Re\{ \cdot b \} \neq \Re\{a\} \cdot \Re\{b\} \quad (23)$$

We can use this algorithm as a guess as to find the form that will work with a real valued waveform. Upon comparison of the Fourier transforms of the complex and real waveforms (see appendix A and B) we see they are very similar. The real looks like the complex with an additional sum of mirrored terms (explain what I mean by this).

What would we have to do to get the fourier transform of the real to look exactly like the fourier transform of the complex wave? Unsurprisingly not much because they are such similar functions. We would only have to

multiply each term by some phase factor to get the real fourier transform to look like the sum of two complex fourier transforms. After adding in the phase factors we plug the fourier transform of the real wave into the Gustafson Algorithm which will yeald two delta functions now instead of one (because the fourier transform of the real is the sum of two complex wave fourier transforms). One delta function will be at $+\omega_0$, this is the one of interest, and the other will be at $-\omega_0$. (A much more rigerous explanation of this is needed.) If we carry the search out over only positive values of ω_0 then we can throw out all terms in red of the fourier transform of the real wave because they are inconsequential to the algorithm. Finally, the phase terms that were added to the fourier transform of the real to make it look like the complex can be encorporated into the Guatafson Algorithm. The only remaining thing to do is multiply the Gustafson Algorithm by two (explain why).

A. Discussion of The Gustafson Algorithm

It is not explicitly obvious how The Gustafson Algorithm, Eq. 22, is able to determin the values $\omega_0, \omega_1, \phi_0, \phi_1, \Gamma$. In this section we seek to make obvious what Eq. 22 can do. First we start with Eq. 22, and plug in the Fourier Transform of the real of the waveform B6.

$$\begin{aligned} h_0 \delta(\omega - \omega_0) &= \sum_{n=-\infty}^{\infty} e^{-in(\widetilde{\phi}_1 + \pi/2)} J_n(\widetilde{\Gamma}) \hat{f}(\omega + n\widetilde{\omega}_1) \\ &= \frac{h_0}{2} \sum_{m,n=-\infty}^{\infty} e^{i(m\phi_1 - n\widetilde{\phi}_1)} J_n(\widetilde{\Gamma}) J_m(\Gamma) \\ &\quad \times \left[e^{i(\phi_0 + (m-n)\pi/2)} \delta(\omega - \omega_0 + n\widetilde{\omega}_1 - m\omega_1) + e^{-i(\phi_0 + (m+n)\pi/2)} \delta(\omega + \omega_0 + n\widetilde{\omega}_1 - m\omega_1) \right] \end{aligned} \quad (24)$$

Bessel functions have the property []

$$\sum_{n=-\infty}^{\infty} J_n(x) J_{n+m}(x) = \delta_m \quad (26)$$

Where δ_m is the Kronecker Delta. []

B. Consequences of Discretizing

-drichlet kernel

III. CARSON'S RULE

Carson's rule can be understood to say that almost all (98 percent) of the power for a frequency-modulated sinusoidal signal is contained within a finite bandwidth B_T , defined by:

$$B_T = 2(\Delta f + f_m) \quad (27)$$

where Δf is the peak deviation of the instantaneous frequency $f(t)$ from the center carrier frequency f_c , and f_m is the highest frequency in the modulating signal.

The important thing to take away from this is that it takes an infinite bandwidth to transmit a phase/frequency modulated signal regardless of how smooth it is, but in practice only a finite bandwidth is needed for an accurate approximation.

IV. VARIOUS COMPLECATIONS THAT NEED TO BE DEALT WITH (DAVID AND COLIN)

-The LIGO data is interrupted (ie. it comes in chunks—it is not a continuous streem of data). How will this be dealt with?

-Estimating the likelihood that any signal we see is truly a discovery and not noise. (Error Analysis)

-Negative frequencies imply the wave is traveling backwards in time. This is not physically realistic. How can we deal with this? The wave we see is real, so in order for the fourier series to be real we need negative frequencies to cancel the imaginary terms.

-Real data obeys the law of causality. That means the signal starts at $t=0$ and $f(t)=0$ for $t \leq 0$. Putting this restriction on our waveform adds an infinite number of higher frequencies to the fourier transform, even though our waveform doesn't truly contain those frequencies. How should this be dealt with? Hardy functions? (Colin)

-Nyquist frequency is defined as half of the sampling frequency and it puts an effective maximum on the frequencies we can detect. Any frequency that exists above the Nyquist frequency will result in aliasing. Specifically the amplitude of any frequency ω_0 higher than ω_N will be "folded over" and be added to the amplitude of its symmetric counterpart ($\omega_0 - \omega_N$). This will result in the measured amplitude of frequencies lower than ω_N having a systematic error component equal to the magnitude of the amplitude of the frequencies greater than ω_N . Assuming that the amplitude of frequencies decays fast enough this systematic error component can be made arbitrarily small by increasing the sampling frequency. An inspection of the sampling frequency used in the experiment will allow us to estimate this systematic error component and put a maximum on its effect.

V. NOISE SOURCES AND DEALING WITH THEM (SAMUEL AKWEI-SEKYERE WILL BE WORKING ON THIS SECTION)

-The signal we are looking for is a very stable wave, it has little phase drift, frequency drift, and amplitude drift on time scales of the order of many periods.

-Much of the noise on the other hand is Quantum Noise, so it is perfectly random. The phase, and amplitude of a certain frequency share an uncertainty relation so the phase and amplitude, by the laws of physics, must drift.

-This means taking the fourier transform over more data will increase the signal to noise ratio.

-Sam will provide a rigorous proof of this.

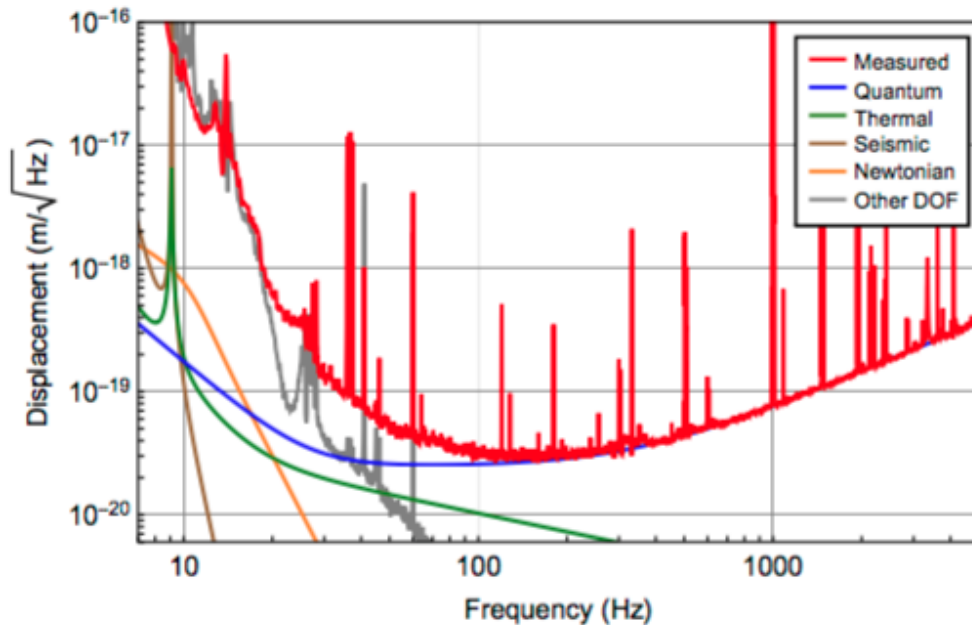


FIG. 2: This plot shows the theoretical noise sources, and the measured noise (red) in the interferometer.

VI. POSSIBLE OTHER AREAS TO REASEARCH

2) The LIGO interferometers sample the data at a finite frequency. This introduces a maximum possible frequency of Gravitational Waves that can be detected, up to the Niquist Frequency. This will, in tern, limit the maximum number of terms we can include in our sum (equation (9)). What is the biggest ω_c , Ω , and Γ that can be reasonably detected? (Task for Fourier Analysis Class MTH 490)

3) Obviously the duration of data is finite. This puts a limit on how finly the Fourier Transform can resolve frequencies, ie. how small frequency bins can be. This in tern tells us how small our step size in ω_c and Ω can be. What are they? (Task for Fourier Analysis Class MTH 490)

4) Over very long periods of time $\omega_c \rightarrow 0$ because the neutron star loses energy/momentum to gravitational wave radation. Over relatively much much shorter time periods Ω and Γ change due to environmental reasons (not entirely sure on this). What limitations does this put on our search, especially if the explicit nature of the time evolution of these parameters is unknown? ANSWER: it shortens the ammount of time we can take data over? (Task for Fourier Analysis Class MTH 490)

7) There are multiple data channels (because there are multiple observatories). Could we compare data channels to help eliminate noise and pick out the exceptionally weak signals?

VII. IMPLEMENTING THE GUSTAFSON ALGORITHM IN C++

A. Calculating Bessel Functions

Known problems with the algorithm include calculating large order bessel functions. The bessel functions of natural number order are given by

$$J_n(z) = \sum_{m=0}^{\infty} \frac{(-1)^m}{m!(m+n)!} \left(\frac{z}{2}\right)^{2m+n} \quad (28)$$

so calculating the nth Bessel function involves calculating factorials greater than n!. The highest n for which we can store n! in an unsigned long integer type, the largest positive integer type, is 20:

$$2^{64} - 1 = 18,446,744,073,709,551,615 \quad (29)$$

$$< 21! = 51,090,942,171,709,440,000 \quad (30)$$

if we are willing to sacrafise some precision to truncation we can use a double precision floating point integer which allows values upto $1.797,693,134,862,315,7 \cdot 10^{308}$

$$170! \approx 7.25 \cdot 10^{306} < 1.797,693,134,862,315,7 \cdot 10^{308} < 171! \approx 1.24 \cdot 10^{309} \quad (31)$$

This is not acceptable however, because $|J_n(z)| \leq 1$, so when performing the sum we need precision all the way down to at the very least 0.1, which would require a mantissa with roughly 308 digits. This is not only impracticle, but it is by far one of the slowest ways one could calculate values of the Bessel functions. This whole buiseness of wresteling with factorials can be avoided by calculating the Bessel Functions using Bessel's Equation 32 [3].

$$x^2 J_n''(x) + x J_n'(x) + (x^2 - n^2) J_n(x) = 0 \quad (32)$$

The standard perscription for numerically solving differential equations is first to discretize the independent variable $x \rightarrow x_i = x_{min} + i \cdot \delta x$. Then use the limit definitions of the derivatives; we will use the three point definitions because their error goes as $O(\delta x^2)$ rather than using the two point definition with an error that goes as $O(\delta x)$ [?]. Also, because there are only one order of Bessel Functions in Bessel's Equation, the order is implied by the n that appears, so we will drop the subscript of n , $J_n \rightarrow J$, and we will further adopt the notation $J(x_i) = J_i$.

$$J'_i = \frac{J_{i+1} - J_{i-1}}{2\delta x} \quad (33)$$

$$J''_i = \frac{J_{i-1} - 2J_i + J_{i+1}}{\delta x^2} \quad (34)$$

So the discretized form of Bessel's Equation is

$$x_i^2 \frac{J_{i-1} - 2J_i + J_{i+1}}{\delta x^2} + x_i \frac{J_{i+1} - J_{i-1}}{2\delta x} + (x_i^2 - n^2) J_i = 0 \quad (35)$$

$$\left(\frac{x_i^2}{\delta x^2} - \frac{x_i}{2\delta x}\right) J_{i-1} + \left(\left(1 - \frac{2}{\delta x^2}\right)x_i^2 - n^2\right) J_i + \left(\frac{x_i^2}{\delta x^2} + \frac{x_i}{2\delta x}\right) J_{i+1} = 0 \quad (36)$$

Where we have collected like terms of J_i . For convenience we define coefficients to simplify the above equation.

$$a_i = \frac{x_i^2}{\delta x^2} - \frac{x_i}{2\delta x} \quad (37)$$

$$b_i = \left(1 - \frac{2}{\delta x^2}\right)x_i^2 - n^2 \quad (38)$$

$$c_i = \frac{x_i^2}{\delta x^2} + \frac{x_i}{2\delta x} \quad (39)$$

These coefficients can be simplified by using the definition for x_i , and taking $x_{min} = 0$.

$$a_i = i \left(i - \frac{1}{2}\right) \quad (40)$$

$$b_i = i^2 (\delta x^2 - 2) - n^2 \quad (41)$$

$$c_i = i \left(i + \frac{1}{2}\right) \quad (42)$$

So the discretized Bessel equation with simplified coefficients is

$$a_i J_{i-1} + b_i J_i + c_i J_{i+1} = 0 \quad (43)$$

Wrighting out the system of equations explicitly:

$$b_1 J_1 + c_1 J_2 = -a_1 J_0 \quad (44)$$

$$a_2 J_1 + b_2 J_2 + c_2 J_3 = 0 \quad (45)$$

$$a_3 J_2 + b_3 J_3 + c_3 J_4 = 0 \quad (46)$$

$$\vdots \quad (47)$$

$$a_{n-1} J_{n-2} + b_{n-1} J_{n-1} + c_{n-1} J_n = 0 \quad (48)$$

$$a_n J_{n-1} + b_n J_n = -c_n J_{n+1} \quad (49)$$

Which suggests Bessel Equation be written as a matrix equation.

$$\begin{pmatrix} b_1 & c_1 & & & \\ a_2 & b_2 & c_2 & & \\ & a_3 & b_3 & c_3 & \\ & & \vdots & \vdots & \\ & & & a_{n-1} & b_{n-1} & c_{n-1} \\ & & & & a_n & b_n \end{pmatrix} \begin{pmatrix} J_1 \\ J_2 \\ J_3 \\ \vdots \\ J_{n-1} \\ J_n \end{pmatrix} = \begin{pmatrix} -a_1 J_0 \\ 0 \\ 0 \\ \vdots \\ 0 \\ -c_n J_{n+1} \end{pmatrix} \quad (50)$$

This is a tridiagonal matrix system that charactorized a one dimentional differential equation. It can be easily solved using the standard Thomas Algorithm. To program this in C++ we need all the arrays to be indexed from 0, so

$$\begin{pmatrix} B_0 & C_0 & & & \\ A_1 & B_1 & C_1 & & \\ & A_2 & B_2 & C_2 & \\ & & \vdots & \vdots & \\ & & & A_{N-4} & B_{N-4} & C_{N-4} \\ & & & & A_{N-3} & B_{N-3} \end{pmatrix} \begin{pmatrix} J_1 \\ J_2 \\ J_3 \\ \vdots \\ J_{N-3} \\ J_{N-2} \end{pmatrix} = \begin{pmatrix} -A_0 J_0 \\ 0 \\ 0 \\ \vdots \\ 0 \\ -C_{N-3} J_{N-1} \end{pmatrix} \quad (51)$$

$$A_i = a_{i+1} = (i+1) \left(i + \frac{1}{2} \right) \quad (52)$$

$$B_i = b_{i+1} = (i+1)^2 (\delta x^2 - 2) - n^2 \quad (53)$$

$$C_i = c_{i+1} = (i+1) \left(i + \frac{3}{2} \right) \quad (54)$$

1. The Thomas Algorithm

The Thomas Algorithm is a lightning fast way to solve tridiagonal systems like equation 51. The algorithm consists of two steps. First there is a forward substitution which eliminates the A_i 's, and modifies the B_i 's and the vector on the right which we will call the source vector S_i ; $\forall i \in [0, N-3]$.

$$R_i = R_i - \frac{A_i}{B_{i-1}} R_{i-1}; \quad \forall i \in [1, N-3] \quad (55)$$

$$B_i \rightarrow B_i - \frac{A_i}{B_{i-1}} C_{i-1}; \quad \forall i \in [1, N-3] \quad (56)$$

$$S_i \rightarrow S_i - \frac{A_i}{B_{i-1}} S_{i-1}; \quad \forall i \in [1, N-3] \quad (57)$$

Then there is a backwards substitution eliminating the C_i 's, again modifying the S_i 's. Finally we solve for J_i .

$$R_i = R_i - \frac{C_i}{B_{i+1}} R_{i+1}; \quad \forall i \in [N-4, 0] \quad (58)$$

$$S_i \rightarrow S_i - \frac{C_i}{B_{i+1}} S_{i+1}; \quad \forall i \in [N-4, 0] \quad (59)$$

$$J_i = \frac{S_{i-1}}{B_{i-1}}; \quad \forall i \in [N-2, 1] \quad (60)$$

The time it takes to perform the Thomas Algorithm goes as N [].

2. Boundary Conditions

To solve this second-order differential equation we will need two boundary conditions. The boundary condition at $x = 0$ is simple.

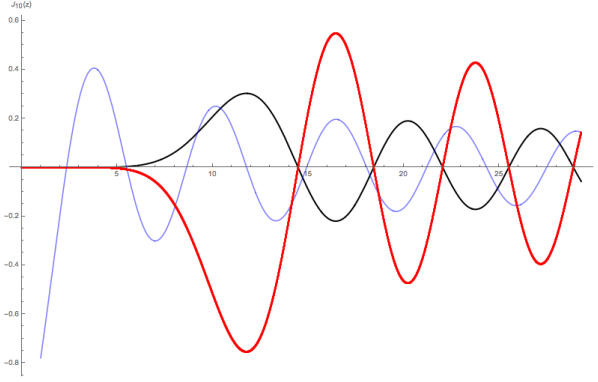
$$J_n(0) = \begin{cases} 1 & : n = 0 \\ 0 & : n \neq 0 \end{cases}$$

For the other boundary condition we *could* use the asymptotic form of the Bessel functions. Theorem 5.1 in [3] states:

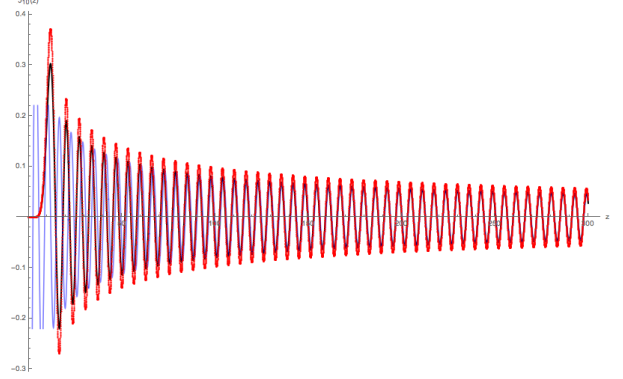
For each $n \in N$ there is a constant $C_n \in R$ such that, if $x \geq 1$, then

$$\left| J_n(x) - \sqrt{\frac{2}{\pi x}} \cos \left(x - \frac{\pi}{4} (2n+1) \right) \right| \leq \frac{C_n}{x^{3/2}} \quad (61)$$

This is an asymptotic expansion, so it is only valid for large values of x . It turns out the accuracy of the solution to bessels equation relies heavily on the accuracy of the endpoint at $x \neq 0$. Figures 3a and 3b illustrate this point quite well. The conclusion is that the asymptotic form of the bessel functions is not accurate enough for even fairly large value of z . We can also do



(a) Notice how the asymptotic form and the one calculated by our differential equation solver match up at the maximum value for z , but do not match up with the true solution. This has far reaching consequences. Whatever multiplicative factor the endpoint is off by seems to carry through for every other point. In this case the multiplicative factor (asymptotic / true) is almost exactly -2.5 . Notice how this inverts the solution and makes it 250% larger.



(b) For much larger values of z the asymptotic form is a better approximation to the true value. In this case the multiplicative factor (asymptotic / true evaluated at $z = 300$) is roughly 1.2 which results in the solution being roughly 20% larger than it should be.

FIG. 3: The blue curve is the asymptotic form of the Bessel functions as given in equation 61, the black curve is $J_{10}(x)$ as given by Mathematica, and the red curve is the one calculated by our differential equation solver. Note, both of these solutions were calculated using 10,000 points. Even though the solution in figure 3a has 10 times the point density, it is limited in accuracy by the endpoint!

$$J_n(z) = \frac{1}{\pi} \int_0^\pi \cos[z \sin \theta - n\theta] d\theta \quad (62)$$

Which is computed using a Riemann Sum

$$J_n(z) \approx \frac{1}{N} \sum_{i=0}^{N+1} \cos[z \sin(i \cdot dx) - n \cdot i \cdot dx]; \quad dx = \frac{\pi}{N} \quad (63)$$

The function being integrated becomes more oscillatory as n increases. Numerical analysis shows that n gives the number of zeros the function has on the interval $(0, \pi)$ for $z = 0$. For $n = 0$ the number of zeros is given by $\text{Floor}(\frac{2z}{\pi})$. We want a way to ensure the calculation is accurate regardless of how oscillatory it is, but we also want it to be as fast as possible, so we use these facts regarding the zeros to ensure there are roughly the same number of integration points between zeros. By taking the number of (evenly spaced) integration points to be

$$N = 100 \cdot (n + 1) \cdot \text{Floor}\left(\frac{2z}{\pi} + 1\right) \quad (64)$$

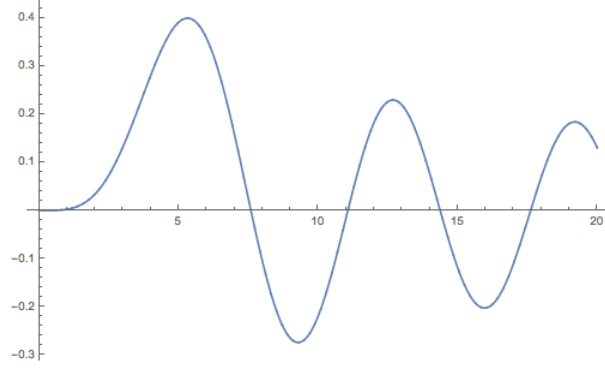
we achieved excellent results (accurate consistently to 16 decimal places) for a wide range of z and n . The +1's are to ensure accurate results when z or n are zero. The algorithm can have problems when J is extremely small. Then the function can be off by many orders of magnitude, but because it is essentially zero, it does not seem to effect our results when used as a boundary condition for solving Bessel's Differential Equation.

3. Calculating Bessel Functions: Results

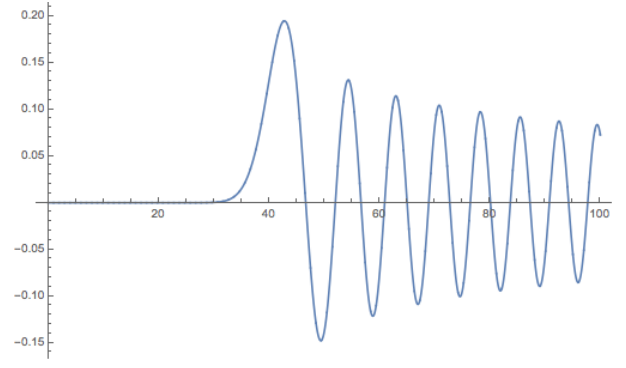
The ultimate benchmark for success in calculating Bessel Functions in this manner (using the Thomas Algorithm to solve Bessel's Differential Equation) is to compare it to the standard way of calculating the value at each point using the Riemann Sum (as defined in equation 63 section VII A 2). So how much faster is it? This depends on the values of n and z because we use a dynamic number of integration points as given by eq. 64. Table I gives the speed increase for various parameters.

Parameters	Point by Point Using Integral	Thomas Algo. Solving Bessel's Equation	Speed Increase
$n = 3$ $N = 500$ $z_{max} = 20.0$	0.051786 s	0.00013800 s	375
$n = 14$ $N = 50,000$ $z_{max} = 100.0$	113.33 s	0.003937 s	28,785

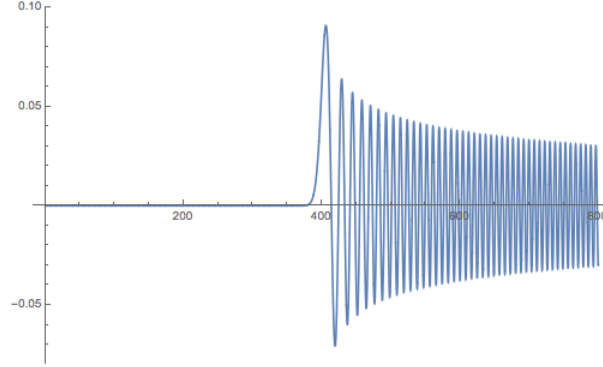
TABLE I: N is the number of points returned, n is the order of the bessel function, and the points calculated were for $z \in [0, z_{max}]$



(a) $n=4$, numPts=10,000, xMax=20, comptime=0.00082



(b) $n=40$, numPts=10,000, xMax=100, comptime=0.00092



(c) $n=400$, numPts=10,000, xMax=800, comptime=0.00200;
About half the computation time went to calculating the endpoint!

FIG. 4

Table 4 gives three examples of Bessel Functions that were calculated using the Thomas Algorithm to solve Bessel's Equation.

VIII. CONCLUSION

Recap the benefits of working in the frequency domain vs the time domain. It is the belief of this author that the methods outlined in this paper are unlikely to be useful for searching for gravitational waves.

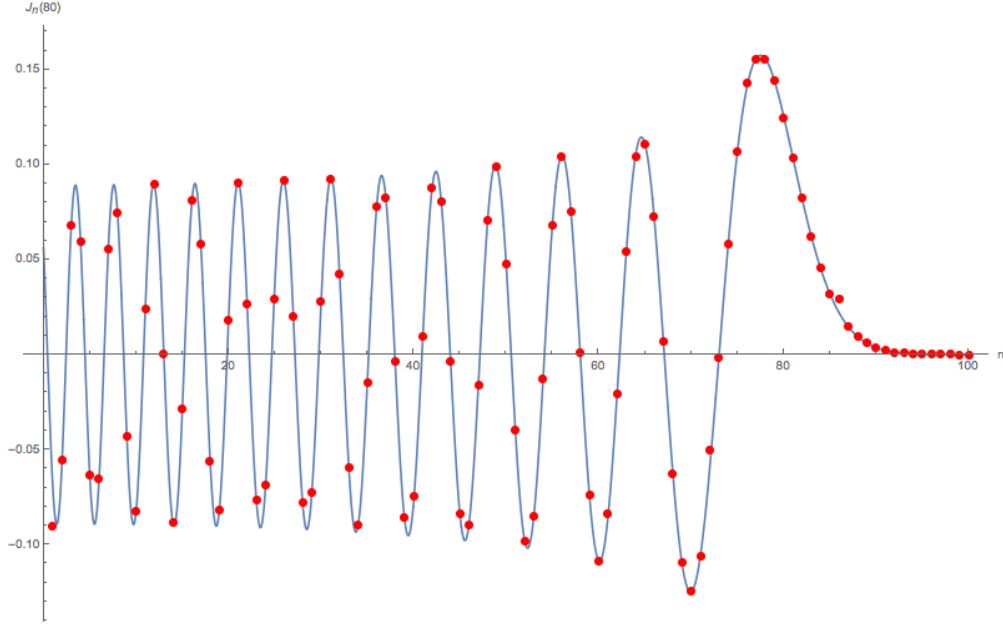


FIG. 5: This plot is a plot of $J_n(80)$ for values of $n \in (0, 100)$. The blue curve was generated by the BesselJ function of Mathematica. The red dots were calculated by my code. The two sets of data are in excellent agreement except perhaps $n = 0, 85$ in which case there is a slight disagreement. This is a small selection of the 400,000 data points my code generated in 0.33 seconds (on 5 year old a laptop). It solved the Bessel differential equation for 4000 steps in $\Gamma \in (0, 100)$, then saves the output, and moved on to solve Bessel's Equation for the next value of n until all values of Γ and n were solved for.

Appendix A: The Fourier Transform of The Complex Function

I BELIEVE I FORGOT SOME FACTORS OF 2PI HERE!! Use the convolution theorem Use the Jacobi-Anger expansion 12 Use the linearity of the Fourier Transform Use the linearity of the Convolution

$$\mathcal{F}_t \left[h_0 e^{i(\omega_0 t + \phi_0 + \Gamma \cos(\omega_1 t + \phi_1))} \right] = h_0 e^{i\phi_0} \mathcal{F}_t \left[e^{i\omega_0 t} e^{i\Gamma \cos(\omega_1 t + \phi_1)} \right] \quad (\text{A1})$$

$$= h_0 e^{i\phi_0} \mathcal{F}_t \left[e^{i\omega_0 t} \right] \star \mathcal{F}_t \left[e^{i\Gamma \cos(\omega_1 t + \phi_1)} \right] \quad (\text{A2})$$

$$= h_0 e^{i\phi_0} \delta(\omega - \omega_0) \star \mathcal{F}_t \left[\sum_{n=-\infty}^{\infty} e^{in\pi/2} J_n(\Gamma) e^{in(\omega_1 t + \phi_1)} \right] \quad (\text{A3})$$

$$= h_0 e^{i\phi_0} \delta(\omega - \omega_0) \star \sum_{n=-\infty}^{\infty} e^{in\pi/2} e^{in\phi_1} J_n(\Gamma) \mathcal{F}_t \left[e^{in\omega_1 t} \right] \quad (\text{A4})$$

$$= h_0 e^{i\phi_0} \delta(\omega - \omega_0) \star \sum_{n=-\infty}^{\infty} e^{in(\phi_1 + \pi/2)} J_n(\Gamma) \delta(\omega - n\omega_1) \quad (\text{A5})$$

$$= h_0 e^{i\phi_0} \sum_{n=-\infty}^{\infty} e^{in(\phi_1 + \pi/2)} J_n(\Gamma) \delta(\omega - \omega_0) \star \delta(\omega - n\omega_1) \quad (\text{A6})$$

$$= h_0 e^{i\phi_0} \sum_{n=-\infty}^{\infty} e^{in(\phi_1 + \pi/2)} J_n(\Gamma) \delta(\omega - \omega_0 - n\omega_1) \quad (\text{A7})$$

Appendix B: The Fourier Transform of The Real-Valued Function

$$\mathcal{F}_t \left[\Re \left\{ h_0 e^{i(\omega_0 t + \phi_0 + \Gamma \cos(\omega_1 t + \phi_1))} \right\} \right] = \frac{1}{2} \mathcal{F}_t \left[h_0 e^{i(\omega_0 t + \phi_0 + \Gamma \cos(\omega_1 t + \phi_1))} + h_0 e^{-i(\omega_0 t + \phi_0 + \Gamma \cos(\omega_1 t + \phi_1))} \right] \quad (\text{B1})$$

$$= \frac{h_0}{2} \left[e^{i\phi_0} \mathcal{F}_t \left[e^{i(\omega_0 t + \Gamma \cos(\omega_1 t + \phi_1))} \right] + e^{-i\phi_0} \mathcal{F}_t \left[e^{i(-\omega_0 t - \Gamma \cos(\omega_1 t + \phi_1))} \right] \right] \quad (\text{B2})$$

From the previous section we see that

$$\mathcal{F}_t \left[e^{i(\omega_0 t + \Gamma \cos(\omega_1 t + \phi_1))} \right] = \sum_{n=-\infty}^{\infty} e^{in(\phi_1 + \pi/2)} J_n(\Gamma) \delta(\omega - \omega_0 - n\omega_1) \quad (\text{B3})$$

and by replacing ω_0 with $-\omega_0$ and Γ with $-\Gamma$, and using the fact that $J_n(-\Gamma) = (-1)^n J_n(\Gamma)$ we also have

$$\mathcal{F}_t \left[e^{i(-\omega_0 t - \Gamma \cos(\omega_1 t + \phi_1))} \right] = \sum_{n=-\infty}^{\infty} e^{in(\phi_1 - \pi/2)} J_n(\Gamma) \delta(\omega + \omega_0 - n\omega_1) \quad (\text{B4})$$

so the Fourier Transform of the real part of our frequency/phase modulated signal is

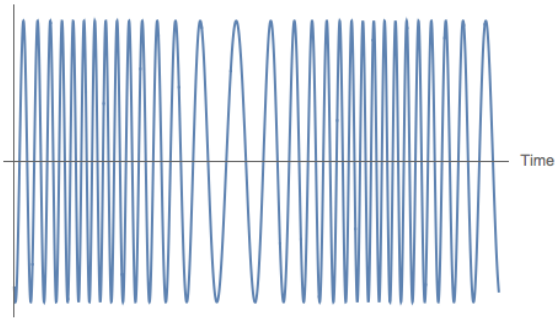
$$\begin{aligned} \mathcal{F}_t \left[\Re \left\{ h_0 e^{i(\omega_0 t + \phi_0 + \Gamma \cos(\omega_1 t + \phi_1))} \right\} \right] &= \frac{1}{2} h_0 \left[e^{i\phi_0} \sum_{n=-\infty}^{\infty} e^{in(\phi_1 + \pi/2)} J_n(\Gamma) \delta(\omega - \omega_0 - n\omega_1) \right. \\ &\quad \left. + e^{-i\phi_0} \sum_{n=-\infty}^{\infty} e^{in(\phi_1 - \pi/2)} J_n(\Gamma) \delta(\omega + \omega_0 - n\omega_1) \right] \\ &= \frac{1}{2} h_0 \sum_{n=-\infty}^{\infty} e^{in\phi_1} J_n(\Gamma) \left[e^{i(\phi_0 + n\pi/2)} \delta(\omega - \omega_0 - n\omega_1) \right. \\ &\quad \left. + e^{-i(\phi_0 + n\pi/2)} \delta(\omega + \omega_0 - n\omega_1) \right] \end{aligned} \quad (\text{B5})$$

$$\frac{1}{2} h_0 \sum_{n=-\infty}^{\infty} e^{in\phi_1} J_n(\Gamma) \left[e^{i(\phi_0 + n\pi/2)} \delta(\omega - \omega_0 - n\omega_1) + e^{-i(\phi_0 + n\pi/2)} \delta(\omega + \omega_0 - n\omega_1) \right] \quad (\text{B6})$$

Notice that, by taking the fourier transform of just the real part of our frequency modulated function it has added the terms in red. (Go into more detail why that is) The other important change is that the X_n and Y_n terms were added (Again, go into more detail why that is).

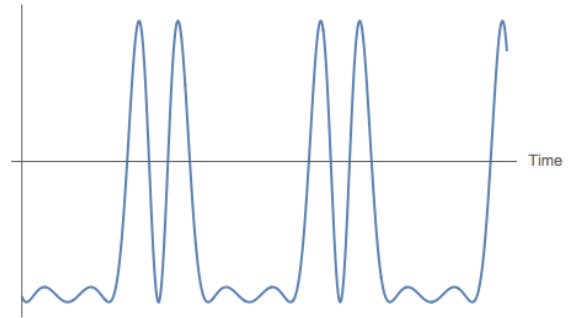
Appendix C: Selected Waveforms

-
- [1] Deanna Emery. A coherent three dimensional fft based search ~~for~~ ^{search for} gravitational waves from binary neutron star systems. *LIGO DCC*, (T1500307-v2), September 2015.
 - [2] B.P. Abbott et al. (LIGO Scientific Collaboration and Virgo Collaboration). Observation of gravitational waves from a binary black hole merger. *Physical Review Letters*, 116(061102):1–16, 12 February 2016.
 - [3] Gerald B. Folland. *Fourier Analysis and its Applications*. Number ISBN 0-534-17097-3. Brooks and Cole Publishing Company, 1992.
 - [4] David J. Griffiths. *Introduction to Quantum Mechanics*. Number ISBN 0-13-111892-7. Pearson, second edition edition, 2005.
 - [5] Peter R. Saulson. *Fundamentals of Interferometric Gravitational Wave Detectors*. World Scientific Publishing Company,



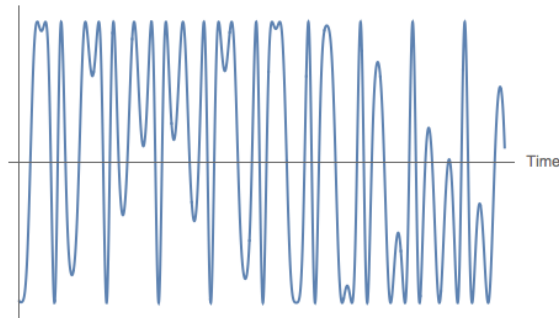
(a) A "nice" signal that is what comes to mind for cyclic frequency modulated signals.

$$\Gamma = 9.88, \omega_0 = 3.62, \omega_1 = 0.21, \phi_1 = 3.14$$



(b) One example of the exotic signals cyclic frequency modulation can produce.

$$\Gamma = 2.88, \omega_0 = 1.5, \omega_1 = 0.75, \phi_1 = 0$$



(c) A particularly nasty waveform that could be mistaken as noise by looking at it. $\Gamma = 3, \omega_0 = 0.42, \omega_1 = 0.46, \phi_1 = 0.1$